

Phonon density of states of superconducting $\text{YBa}_2\text{Cu}_3\text{O}_7$ and the nonsuperconducting analog $\text{YBa}_2\text{Cu}_3\text{O}_6$

J. J. Rhyne, D. A. Neumann, J. A. Gotaas, and F. Beech
*Institute for Materials Science and Engineering, National Bureau of Standards,
Gaithersburg, Maryland 20899*

L. Toth and S. Lawrence
Ceramics Branch, Naval Research Laboratory, Washington, D.C. 20375

S. Wolf, M. Osofsky, and D. U. Gubser
Metal Physics Branch, Naval Research Laboratory, Washington, D.C. 20375
(Received 6 May 1987; revised manuscript received 18 June 1987)

Neutron scattering has been used to study the vibrational density of states and the atomic structure of the high-temperature superconductor $\text{YBa}_2\text{Cu}_3\text{O}_7$, and the analogous nonsuperconducting compound $\text{YBa}_2\text{Cu}_3\text{O}_6$. The density of states of the superconductor shows a strong double peak at about 20 meV and a second major maximum near 70 meV with additional less-intense features present at intermediate energies. The $\text{YBa}_2\text{Cu}_3\text{O}_6$ material shows a similar energy spectrum above 45 meV; however, below this energy there are significant differences associated with the O vacancies in the linear b -axis chain site.

The discovery of superconductivity above 90 K by Wu *et al.*¹ in a polyphase sample of composition $\text{Y}_{1.2}\text{Ba}_{0.8}\text{CuO}_y$ and the subsequent identification of the superconducting phase² has prompted intense efforts to determine the properties of this and analogous compounds in the Y-Ba-Cu-O phase diagram. In this Brief Report we present inelastic neutron scattering results on the superconducting material $\text{YBa}_2\text{Cu}_3\text{O}_7$ and on the nonsuperconducting but crystallographically equivalent compound $\text{YBa}_2\text{Cu}_3\text{O}_{6.05}$.

The samples used were prepared at the Naval Research Laboratory from 99.9% purity starting materials of Y_2O_3 , CuO , and BaCO_3 and were of nominal composition $\text{YBa}_2\text{Cu}_3\text{O}_x$. The powders were predried to remove adsorbed H_2O and then premixed carefully to break up agglomerates. The premixed powders were calcined at temperatures of 900–950°C for a period of 6 h with hourly intermediate regrindings. The degree of chemical reaction was monitored by x rays. The calcined powders were then ground and cold pressed into pellets of 1–2 gm size and sintered for 12 h at 937°C. The samples were finally annealed under oxygen at 900°C for 3 h and then furnace cooled at 1° per minute to 300°C before removal from the furnace. Individual pellets were characterized with x-ray diffraction and found to be identical.

The samples were examined for superconductivity by four-probe resistance measurements and by dc susceptibility. The resistance data showed the first deviation from a linear temperature dependence at temperatures in excess of 115 K. Between 115 and 93 K the sample resistance drops by about 10% from a straight line extrapolation of the high- T data. At 93 K the resistance drops sharply and the sample is fully superconducting at 91 K.

The oxygen site occupation was determined by the technique of total profile refinement applied to neutron powder

diffraction data taken on the five-detector powder instrument at the National Bureau of Standards Reactor. The data were analyzed in the orthorhombic space group $Pnmm$ as reported by Beech, Miraglia, Santoro, and Roth³ for a sample of the $\text{YBa}_2\text{Cu}_3\text{O}_7$ compound prepared by a similar procedure and having similar superconducting properties. This refinement produced nearly identical lattice parameters ($a_0=3.8220$ Å, $b_0=3.8855$ Å, and $c_0=11.6797$ Å) and atomic coordinates to those of Ref. 3. Refinement of the site occupation factors led to a stoichiometry $\text{YBa}_2\text{Cu}_3\text{O}_{6.95}$ for this sample, with an uncertainty of 0.01 in the oxygen composition. The essential features of the oxygen site occupancy are the complete filling of three of the four oxygen positions, with the vacancies all occurring in the [O(4)] site which occurs in a linear chain along the b axis alternated with Cu(1) atoms. Thus this site is occupied in the proportional fraction of unit cells and empty in the remainder. It should be noted that the thermal factor for this site is larger by more than a factor of 2 than those for the other oxygen sites, consistent with large fluctuations (static and/or dynamic) of these oxygen atoms.

The O_6 material was prepared by a post anneal in flowing argon at 750°C for 15 h. This lowered the oxygen content to 6.05 atoms. As found in the study by Santoro *et al.*,⁴ the oxygen deficiency, determined from a total profile refinement of the powder diffraction data, is entirely associated with the O(4) linear chain site. No superconducting transition was found in these samples.

Neutron diffraction yields unique structural information, due to its strong sensitivity to oxygen scattering; and likewise inelastic neutron scattering provides a direct determination of the vibrational modes which may be crucial to understanding the superconductivity mechanism in these compounds. It would be preferable to determine the

complete phonon dispersion relation, particularly in light of the highly anisotropic conductivity properties which these materials display; however, single crystals of sufficient size for such a measurement are not available. Therefore, measurements are currently limited to the wave-vector (q) averaged phonon density of states obtained from a powder sample.

The vibrational density of states was obtained from the inelastic neutron scattering data using the incoherent approximation; that is, we have assumed that the dynamic coherent scattering function can be replaced by its incoherent counterpart.^{5,6} Within this formalism, the scattering function is given by⁷

$$\frac{d^2\sigma}{d\Omega d\omega} \propto \frac{k'}{k} \frac{n(\omega)+1}{\omega} \left(\sum x_i I_i(\omega) g_i(\omega) \right), \quad (1)$$

where $I_i(\omega)$ is defined by

$$I_i(\omega) = \frac{\sigma_i}{m_i} \langle (\mathbf{Q} \cdot \boldsymbol{\epsilon}_i)^2 e^{-2W_i} \rangle. \quad (2)$$

Here k and k' are the magnitudes of the incident and final neutron wave vectors, \mathbf{Q} is the scattering vector, $n(\omega)$ is the Bose occupation factor for a vibrational state of energy ω , and x_i , m_i , σ_i , and $\boldsymbol{\epsilon}_i$ are the atomic concentration, nuclear mass, total scattering cross section, and displacement vector of the i th atomic species, respectively; W_i is the Debye-Waller factor, which was assumed to be negligible at the sample temperatures in this study, and the angle brackets indicate that an average has been taken over all sites of type i and over all modes of energy ω . Finally, $g_i(\omega)$ represents the density of states for the i th constituent, which is defined by

$$g_i(\omega) = \sum_{\beta} \delta(\omega - \omega_{i,\beta}), \quad (3)$$

where the sum is taken over all normal modes. Therefore, the scattering does reflect the phonon density of states; however, the contributions from the different species are weighted by the values of $I_i(\omega)$. From Eq. (2) one sees that the important quantity in determining this weighting is the total scattering cross section divided by the mass. For O, Cu, Ba, and Y these values are 0.26, 0.12, 0.043, and 0.08 (barns/amu), respectively. Thus $\approx 80\%$ of the observed scattering will be due to vibrations of the oxygen atoms.

The inelastic neutron scattering data were collected using a triple-axis instrument located at the National Bureau of Standards reactor. The low-energy portion ($\omega \leq 25$ meV) of the density of states was obtained using the constant Q mode with a fixed final energy of 13.8 meV. Pyrolytic graphite [(002) reflection] was used for both the monochromator and analyzer and a graphite filter was placed in the scattered beam to remove harmonic contamination. The collimation was 40'-40'-40'-80', yielding a resolution of about 1-3 meV in the range of energy transfers probed with the triple-axis configuration. Data were taken at several values of the scattering vector between 3.3 and 5.0 \AA^{-1} and then averaged in order to assure that the incoherent approximation was indeed satisfied.

The higher-energy data (> 20 meV) were taken using

a Be-graphite-Be filter analyzer assembly. In this case, the analyzer was fixed at a scattering angle of 90° allowing Q to vary as a function of energy. Data were collected between 20 and 40 meV with a graphite monochromator and collimation of 40'-20', yielding energy resolutions between 2 and 3 meV. At larger energy transfers (33 meV $\leq \omega \leq 130$ meV), a Cu monochromator [(220) reflection] was used with a collimation of 60'-40', thereby giving a resolution of 2-6 meV. No collimation was placed after the sample, thus yielding some averaging over the scattering vector, despite the fact that data were collected at only one average scattering angle. In addition, the scattering vector was relatively large, thereby minimizing the effects due to coherent scattering. Considering these factors and the results of previous neutron scattering studies concerning the density of states of coherent scatterers,⁷⁻⁹ we conclude that any effects due to coherent scattering will only be manifested in the relative intensities of the various features and that they will affect the relative intensities by at most 25%, or approximately the size of the error bars.

The contribution to the scattering from the fast neutron background was measured and subtracted directly. The scattering from the sample can was measured and found to be negligible. Multiphonon and multiple scattering corrections were obtained by extrapolation from energies where one phonon scattering is absent. The data were also corrected for all of the energy-dependent factors given in Eq. (1). Then, using the overlapping energy regions as a guide, the density of states obtained in the three different energy ranges was scaled to obtain a single density of states, which was then normalized so that the integrated density of states was unity.

The neutron weighted phonon density of states, $\bar{g}(\omega)$, of YBaCu₃O₇ at 120 K is shown in Fig. 1. Below 9 meV, $\bar{g}(\omega)$ displays the typical ω^2 dependence characteristic of three-dimensional systems. At an energy of about 12 meV, there is a small shoulder most probably due to a zone-boundary interlayer shear model. The density of states then further increases, reaching a large maximum

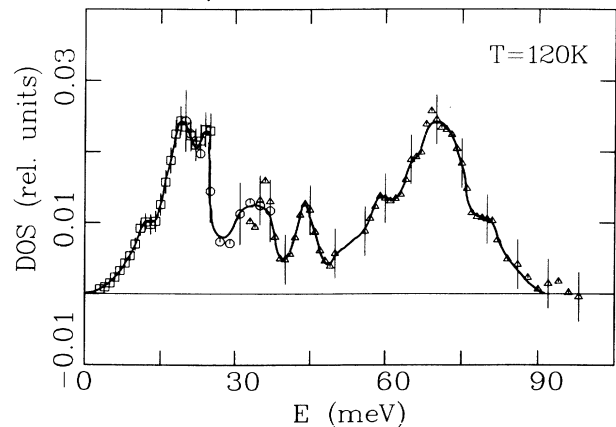


Fig. 1. Vibrational density of states as measured with inelastic neutron scattering at 120 K. The largest spectral weight is contained in peaks involving oxygen vibrations (see text).

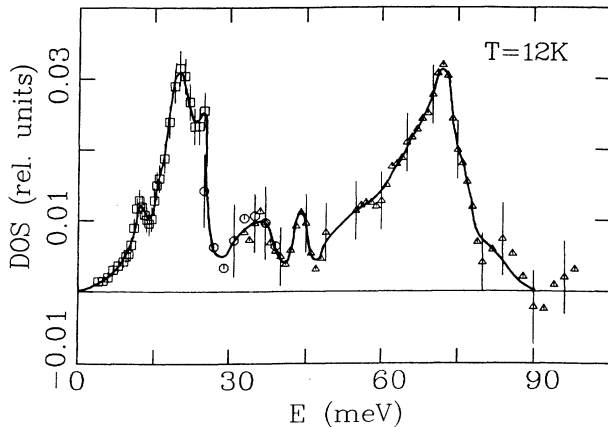


FIG. 2. Density of states at 12 K illustrating the nearly negligible shifts occurring on cooling below the superconducting transition temperature.

at 19–20 meV, followed by another maximum at roughly 25 meV, before dropping precipitously to a minimum at 28–30 meV. There is then a broad feature centered at about 34 meV, and at an energy of 44 meV, the data displays another small maximum which is somewhat narrower than the feature at 34 meV. Above meV, $\bar{g}(\omega)$ increases to a shoulder at about 60 meV and then a peak at 70 meV before dropping to zero at about 90 meV.

The scatter of the data in the E range at about 35 meV made the scaling of the spectra difficult and introduced some uncertainty in the relative heights of the low- and high-energy portions of the density of states. The different symbols represent data collection modes discussed earlier, and indicate that the scaling which we have chosen is certainly reasonable. The data which is omitted around 53 meV corresponds to a region of anomalous transmission of the filter analyzer, making it impossible to determine the density of states for these points. It is noted

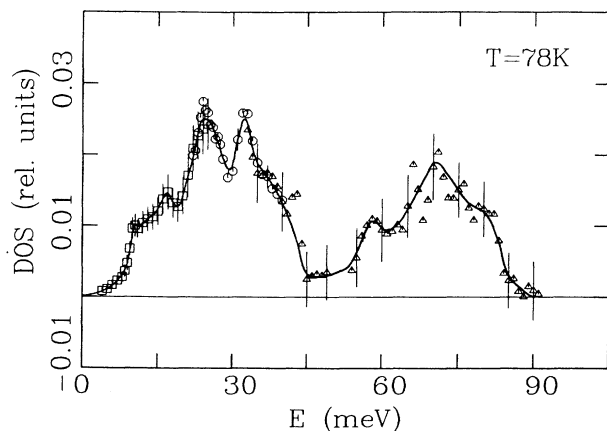


FIG. 3. Vibrational density of states for the nonsuperconducting control compound $\text{YBa}_2\text{Cu}_3\text{O}_6$ measured at 78 K. The scattering about 45 meV is essentially unchanged from the superconducting material, while that at lower energies shows significant changes in relative weights of the peaks.

that the high-energy modes certainly involve the O atoms, thereby increasing their relative weight in the scattering. Thus the rather unusual relative height of the low-energy and the high-energy density of states peaks is due to the degree of O-atom participation in the modes in these energy regions.

We have also measured the density of states in the superconducting state at a temperature of 12 K, as shown in Fig. 2. The only difference which we were able to clearly discern was a slight shift (roughly $\frac{1}{2}$ –1 meV) in the energy range of 10–20 meV which can be accounted for by rather typical anharmonic effects. All other differences were so slight that they may easily have been due to slight differences in the corrections applied to the data.

In contrast, the density of states of the nonsuperconducting $\text{YBa}_2\text{Cu}_3\text{O}_6$ compound shows significant differences in the spectrum, particularly in the relative weights of the peaks in the energy range below about 45 meV. As observed in Fig. 3, the high-energy feature (≈ 70 meV) is essentially the same for the nonsuperconducting compound as for the $\text{YBa}_2\text{Cu}_3\text{O}_7$, and as a result probably represents vibrational states associated with the planar and tetrahedral oxygen sites [O(1), O(2), and O(3)] which have not changed their occupancy. This is consistent with the recent speculation of Hemley and Mao¹⁰ that the mode at about 60 meV is associated with a Cu-O(1) breathing mode. The double peak structure at 19 to 25 meV is dramatically different in the nonsuperconducting material. In the nonsuperconductor, the relative height of the density of states feature at 19 meV has been strongly reduced compared to the one at 25 meV. The scattering minimum near 30 meV is common to both materials; however, the broad, relatively weaker feature around 34 meV in the superconductor has become a dominant peak in the nonsuperconductor with shoulder scattering extending out to include the peak near 44 meV. Another minimum occurs around 47 meV in both materials. It is thus suggestive that the scattering between about 25 and 45 meV reflects optic modes involving the copper and oxygen atoms with polarization vectors in the plane, since these would certainly be affected by the removal of oxygen atoms from the O(4) site. Recent far-infrared measurements¹¹ have revealed a slight energy shift of the peaks in this energy region upon cooling $\text{YBa}_2\text{Cu}_3\text{O}_7$ through the superconducting transition temperature. Raman spectra on a $\text{EuBa}_2\text{Cu}_3\text{O}_7$ sample¹² in the energy range from 45 to 85 meV show strong phonon peaks at 60 and 77 meV with weaker features at 52 and 70 meV. In their range of overlap, these data agree with the peak energies found for $\text{YBa}_2\text{Cu}_3\text{O}_7$ in the present neutron scattering results.

In the absence of a complete model calculation, it is not possible to make a definitive assignment of specific vibrational modes to the observed peaks in the density-of-states spectrum. However, as stated above, the overall spectrum is dominated by oxygen atom modes, and those arising from the O(4) linear chain site contribute to the lower-energy peaks in the spectrum and do not contribute strongly to the major features above 45 meV, which remain unaffected by removal of more than 90% of the oxygen from the O(4) site.

The authors have benefited extensively from discussions with J. J. Rush on the density-of-states measurements and with A. Santoro and S. Miraglia on the structure determination. We also appreciate their help in the crystal structure refinement and the use of their results prior to publication.

-
- ¹M. K. Wu, J. R. Ashburn, C. J. Torng, P. H. Hor, R. L. Meng, L. Gao, Z. J. Huang, Y. Q. Wang, and C. W. Chu, *Phys. Rev. Lett.* **58**, 908 (1987).
- ²R. J. Cava, B. Batlogg, R. B. van Dover, D. W. Murphy, S. Sunshine, T. Siegrist, J. P. Remeika, E. A. Rietman, S. Zuhurah, and G. P. Espinosa, *Phys. Rev. Lett.* **58**, 1676 (1987).
- ³F. Beech, S. Miraglia, A. Santoro, and R. S. Roth, *Phys. Rev. B* **35**, 8778 (1987).
- ⁴A. Santoro, S. Miraglia, F. Beech, S. A. Sunshine, D. W. Murphy, L. F. Schneemeyer, and J. V. Waszczak, *Mater. Res. Bull.* (to be published).
- ⁵M. M. Bredov, B. A. Kotov, N. M. Okuneva, V. S. Oskotskii, and A. L. Shakh-Bugadov, *Fiz. Tverd. Tela. (Leningrad)* **9**, 287 (1967) [*Sov. Phys. Solid State* **9**, 214 (1967)].
- ⁶V. S. Oskotskii, *Fiz. Tverd. Tela (Leningrad)* **9**, 550 (1967) [*Sov. Phys. Solid State* **9**, 420 (1967)].
- ⁷N. Lustig, J. S. Lannin, J. M. Carpenter, and R. Hasegawa, *Phys. Rev. B* **32**, 2778 (1985).
- ⁸N. Maley, J. S. Lannin, and D. L. Price, *Phys. Rev. Lett.* **56**, 1720 (1986).
- ⁹P. F. Miceli, S. E. Youngquist, D. A. Neumann, H. Zabel, J. J. Rush, and J. M. Rowe, *Phys. Rev. B* **34**, 8977 (1986).
- ¹⁰R. J. Hemley and H. K. Mao, *Phys. Rev. Lett.* **58**, 2340 (1987).
- ¹¹D. A. Bonn, J. E. Greedan, C. B. Stager, T. Timusk, M. G. Doss, S. L. Herr, K. Kamaras, and D. B. Tanner, *Phys. Rev. Lett.* **58**, 2249 (1987).
- ¹²B. Batlogg, R. J. Cava, A. Jayaraman, R. V. van Dover, G. A. Kourouklis, S. Sunshine, D. W. Murphy, L. W. Rupp, H. S. Chen, A. White, K. T. Short, A. M. Muzsca, and E. A. Rietman, *Phys. Rev. Lett.* **58**, 2333 (1987).